Collimated Plasmon Beam: Nondiffracting versus Linearly Focused

L. Li, T. Li,* S. M. Wang, and S. N. Zhu

National Laboratory of Solid State Microstructures, School of Physics, College of Engineering and Applied Sciences, Nanjing University, Nanjing 210093, China

(Received 4 September 2012; revised manuscript received 22 November 2012; published 25 January 2013)

We worked out a new group of collimated plasmon beams by the means of in-plane diffraction with symmetric phase modulation. As the phase type changes from 1.8 to 1.0, the beam undergoes an interesting evolution from focusing to a straight line. Upon this, an intuitive diagram was proposed to elucidate the beam nature and answer the question of whether they are nondiffracting or linear focusing. Based on this diagram, we further achieved a highly designable scheme to modulate the beam intensity (e.g., ''lossless'' plasmon). Our finding holds remarkable generality and flexibility in beam engineering and would inspire more intriguing photonic designs.

DOI: 10.1103/PhysRevLett.110.046807 PACS numbers: 73.20.Mf, 42.25.Fx, 78.67.−n

Surface plasmon polariton (SPP) is a combined excitation of an electron and photon, which provides a possible solution to integrate the light at a subwavelength scale and suggests many charming applications [1]. Among various research, a nondiffracting SPP beam is both of fundamental interest and useful functionality (e.g., guiding surface waves). As the counterpart of optical Airy beam in free space [2,3], the realization of Airy plasmon provides a good solution to achieve a nondiffracting surface wave without any nonlinearity [4–8]. Actually, beam engineering has attracted increasing interest nowadays (e.g., arbitrary convex trajectories [9,10], in the nonparaxial region [11–13]). Another aspect of high interest is the beam focusing that reflects the capability of people to concentrate the optical field, which has already received extensive studies in the plasmonic regime [14–17]. In some sense, the nondiffracting beam can be regarded as a particular kind of focusing with a preserved focal spot as the beam propagates, and it is worthwhile to engineer elaborately. However, the well demonstrated Airy plasmon would not always be convenient in on-chip integrations for its bending trajectory. To generate a straight SPP beam with strong field confinement and controllable intensity is of great importance.

In principle, a straight nondiffracting plasmon beam can be formed by the interference of two intersecting plane waves with a linear wave-front phase (just like the generation of the Bessel beam in free space [18]), which was indeed realized by Lin *et al.* very recently [19]. However, this linear phase is quite different from the 1.5-power phase type of the nondiffracting Airy beam. By carefully investigating them together with the previous focusing case [17], we would find it should attribute to a distinct feature of the Airy beam—asymmetric as the 1.5-power phase in $x < 0$ while there is exponential decay in $x > 0$ [20]. Thereafter, a straightforward question arises about using a symmetric 1.5-power phase to generate a straight nondiffracting SPP beam. If yes, it would possibly open up a new avenue to engineer nondiffracting beams. If not, what is the contribution of different phases and what kind of beam will be constructed?

In this Letter, we utilize the nonperfectly matched (NPM) Bragg diffraction method [7] to establish arbitrary SPP beams with symmetric phase modulation as its type from 1.8 to 1.0. Self-collimated SPP beams are well characterized by leakage radiation microscopy (LRM), which is a well developed technique using an oil-immersed objective to extract the SPPs of large k vectors [21,22]. In some cases, these straight SPP beams appear to be less dispersive till collapse at certain distances. Meanwhile, they also look like the elongated focal spots. So, we raise a paradox of the beams: nondiffracting or focusing to a line? An intuitive diagram is proposed to illustrate the physical insight into this kind of beams with respect to different phase modulations. Based on this, a highly designable scheme is developed in a general sense with the capability of achieving a beam with a required intensity profile, by which an interesting ''lossless'' SPP beam is realized as an example. The new insight and full understanding of the beams are highlighted, and possible applications are discussed.

The strategy to modulate the SPP beam phase by NPM diffractions of a nonperiodic nanocave array has been illustrated in detail [7]. Briefly, when an SPP beam passes through a nanoarray, it will be diffracted to various directions by local units for constructive interference, resulting in an extra 2π phase change between every neighboring row. By careful design, a well diffracted SPP beam with desired lateral phase modulation is accessible. Figure 1(a) schematically shows the SPP diffraction by nonperiodic array, where different optimum diffractions correspond to different units with different angles θ for constructive interference. According to the phase distribution in the x axis, $\phi_m(x) = \phi_0 + k_{\mathrm{spp}}x - 2m\pi$ (ϕ_0 is a reference phase of the incident wave and m is the sequence number of the lattice point), we are able to achieve any required phase type in a general form as $\psi(x) = -cx^n$.

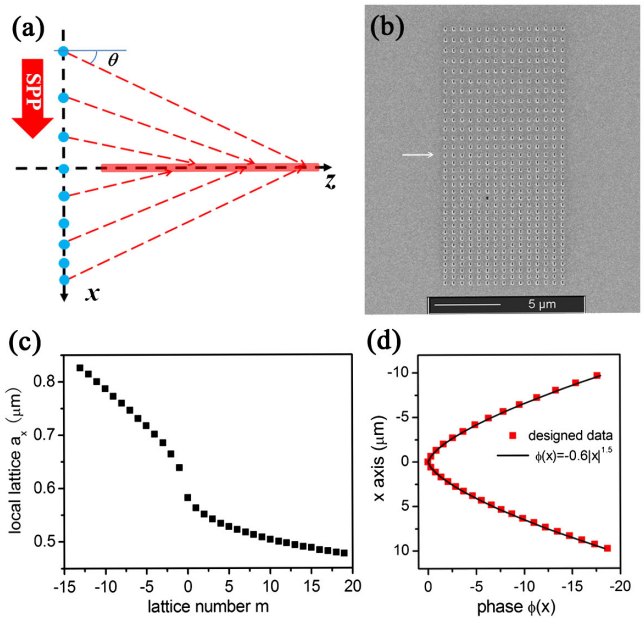

FIG. 1 (color online). (a) Scheme of the generating collimated SPP beam by in-plane diffractions. (b) SEM image of the nonperiodic nanohole array, where an arrow is marked to indicate the symmetric center of the phase modulation. (c) Designed local lattice data a_x. (d) Retrieved phase distribution in lateral dimension of the beam (square symbol) compared with the designed phase type (solid curve).

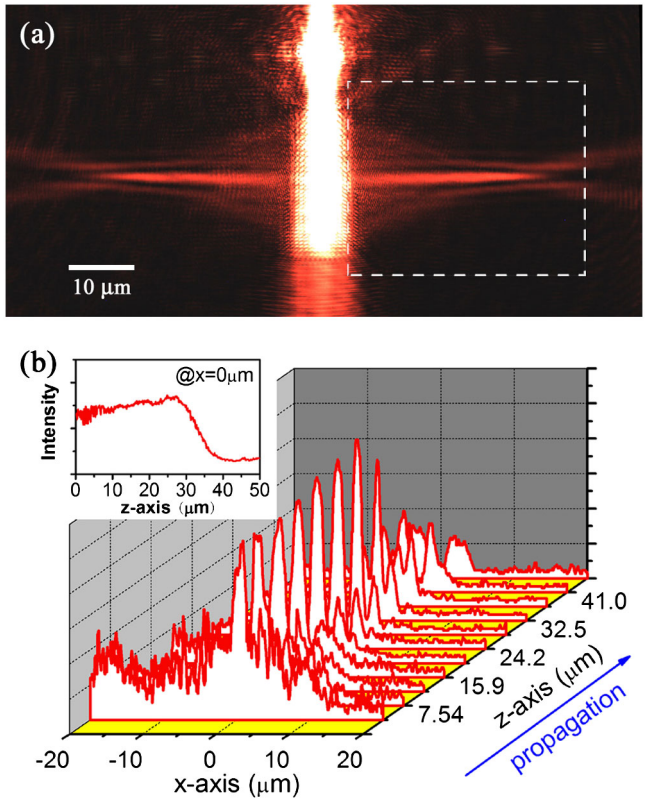

FIG. 2 (color online). (a) LRM recorded SPP beam propagations as diffracted by the well designed nanoarray. (b) Detailed beam cross sections within the selected region in (a), inside which an inset image depicts the beaming profile of the center main lobe.

First, we start from a symmetric $n = 1.5$ phase modulation with a nanoarray covering a wider range of the local lattice in the x direction (a_x) from 826 to 477 nm. The detailed parameters were calculated by solving $\phi_m(x) = \psi(x)$ (with $c = 0.6$) as depicted in Fig. 1(c). The retrieved phase distribution along the x axis shown as symbols in Fig. 1(d) is consistent with the designed one (solid curve). Having these data, we fabricated the sample by focus ion beam (Strata FIB 201, FEI Company) milling on a silver film with ~60 nm thickness on a quartz substrate. Figure 1(b) shows the scanning electron microscopy (SEM) image of the sample, where the unit is a rectangular nanohole with a size of 240×120 nm^2, depth of 20 nm, and local lattice of a_x in Fig. 1(c) and P_z of 610 nm. A white arrow in the figure indicates the symmetric position ($x = 0$), where the local lattice matches the Bragg condition ($a_x \sim 610$ nm), and the lengths of the array in $\pm x$ directions are almost the same (both ~9.7 μm).

The experiment was carried out with an illumination of the He-Ne laser ($\lambda_0 = 632.8$ nm), and the SPP wave was launched by a grating with a period of 610 nm according to the SPP wavelength. Figure 2(a) shows the LRM recorded bidirectional SPP beams, revealing apparent straight collimation of the center lobes. To give more detailed information, beam intensities of cross sections within the selected region [in Fig. 2(a)] are plotted in Fig. 2(b), where a nearly nondispersive peak is well demonstrated with the FWHM kept ~1.5 μm within ~30 μm distance till it vanishes. Interestingly, the peak intensity experiences a slight increase to an abrupt drop as shown in the inset image. Theoretical calculation was subsequently performed on an SPP beaming with a well designed $n = 1.5$ phase with an SPP attenuation length of ~15 μm [7], as the result shown in Fig. 3(a). Both the beam trajectory and beam profile (inset image) reproduce well the experimental results. Since the designed phase is symmetric, it is ready to accept that constructive interference always occurs in the center line. However, this interesting beam intensity profile would likely imply the underlying physics.

As has been illustrated in NPM Bragg diffraction [7], a different local lattice will lead to an optimum diffraction angle θ [see Fig. 1(c)]. This angle can be derived from the differential of the phase function [23], as

$$\sin\theta = -\frac{1}{k}\frac{\partial\psi(x)}{\partial x} = \frac{cn}{k}x^{n-1} \tag{1}$$

by adopting $\psi(x) = -cx^n$. Thereafter, we can easily get the relation of a beam region in the z axis and the corresponding sources region (diffraction units) in the x axis as

$$z = x\cot\theta = \sqrt{\left(\frac{k}{cn}x^{2-n}\right)^2 - x^2}. \tag{2}$$

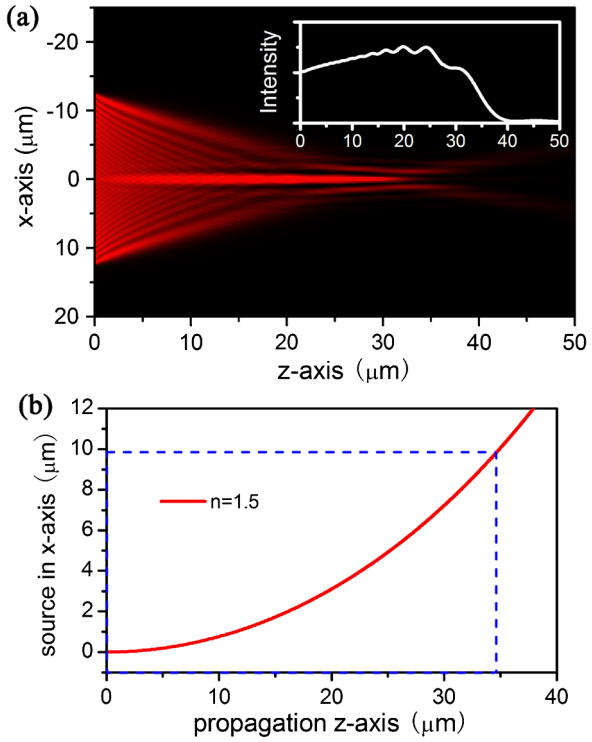

FIG. 3 (color online). (a) Calculated SPP beam with symmetric phase type $n = 1.5$, where the inset image shows the intensity profile of the main lobe. (b) Source-to-beam correspondence curve in the x-z diagram, in which the dashed blue line indicates the region of the finite sources.

Calculating Eq. (2) with $n = 1.5$ and $c = 0.6$, we obtained a diagram of the correspondence curve of the beam in the z axis and the source in the x axis, as shown in Fig. 3(b). An apparent increasing slope of the curve indicates more sources contribute as the beam propagates, suggesting an enhanced beam in propagation. On the other hand, since the designed array is finite ($-9.7 < x < 9.7$ μm), there is no source out of this range [indicated by dashed lines in Fig. 3(b)] to contribute to the beam, which thus leads to an abrupt drop in beam intensity at $z \sim 34$ μm.

For a straightforward generalization, we explored other cases of the phase type changing from $n = 1.8$ to 1.0. Figures 4(a)–4(d) show the results of samples with fixed $c = 0.6$ and $n = 1.8$, 1.6, 1.4, and 1.2, respectively. A clear evolution from a strong focusing to a nearly nondiffracting beaming is demonstrated. Notably, the case of $n = 1.0$ with $c = 1.5$ is particularly shown in Fig. 4(e) (c is changed for a better visualized image), where a nondiffracting beam is clearly observed with the preserved beam shapes, shown in Fig. 4(f). Correspondingly, we calculated their source-to-beam diagrams in order to get an in-depth recognition of these beams, as the results shown in Fig. 4(g). Except for the linear case of $n = 1.0$, others all have an increased tendency in their x-z curves, and the larger n, the larger the increment. The same as the previous $n = 1.5$ case, there is a cutoff in the main lobe due to the

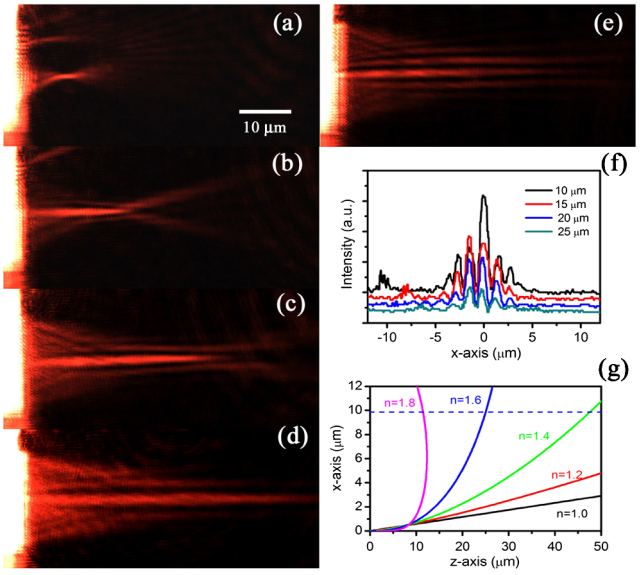

FIG. 4 (color online). (a)–(e) LRM recorded SPP beam with the diffracted phase modulation of $n = 1.8$, 1.6, 1.4, 1.2, and 1.0, respectively ($c = 1.5$ for $n = 1.0$ and $c = 0.6$ for others, and all in same scale). (f) Recorded beam shapes ($n = 1.0$) at different distances (10, 15, 20, 25 μm, from top to bottom). (g) Source-to-beam correspondence curves for all cases, in which the finite source region is indicated by the blue dashed line.

finite array region, as indicated by a dashed line of $x = 9.7$ μm. It does explain the experimental results. However, for the case of $n = 1.8$, we will find that no matter how large the source provided is, the beam range is limited, and most sources only contribute to a narrow region around $z \sim 10$ μm. In this regard, it appears to be a focusing process. However, does it mean that the smaller n cases truly correspond to infinite beaming as long as the sources are infinite?

Revisiting Eq. (2), we will find it can be renormalized for some particular cases. For example, when $n = 1$ it degenerates to a line with a slope of $\sqrt{(\frac{k}{cn})^2 - 1}$; when $n = 1.5$ it becomes a circle equation with a radius of $r = \frac{1}{2}(\frac{k}{1.5c})^2$ and a center of $(r, 0)$; when $n = 2$ it is still a circle with $r = k/2c$ and a center of (0, 0) (see the Supplemental Material [24]). It is clear that the x-z curve for $n = 1.5$ in Fig. 3(b) is just a part of the circle arc, which implies the main lobe of beam will not go farther than the radius ($z = r = 65.4$ μm) even if the source is infinite. As for other cases, the calculated correspondence x-z curves reveal that their curvatures are determined by the coefficient c and phase factor n. It is evident that these curves only cover a finite region in the z dimension except for the $n = 1.0$ case (see the Supplemental Material). In fact, the $n = 1.0$ phase type truly corresponds to the case of two crossing SPP plane waves with the result of a nondiffracting cosine-Gauss beam [19]. Again in Fig. 4(g), the straight x-z line of the $n = 1.0$ case does indicate an equal contribution of sources to the beam everywhere, which is also the nature of

the nondiffracting beam. However, the experimental result definitely shows us a decay beam, which is rightly because of the plasmonic loss as well as in Ref. [19]. Now, it is well recognized that beams of the phase type $n \neq 1$ are not nondiffraction since they are all limited within a certain range. However, the small n cases have revealed the nearly nondiffracting characteristic and weaker side lobes if they are carefully designed. In this regard, these self-collimated beams are able to work as the nondiffracting one to some extent. It does provide a robust method to generate a straight SPP beam with a preserved narrow beamwidth, which holds more generality for further manipulations.

Furthermore, a highly designable scheme is developed to retrieve an arbitrary phase to achieve a desired beam intensity profile. As we know, the SPP wave always suffers from the large propagation loss even for the nondiffracting cosine-Gauss beam [19]. Our design has already manifested the capability to compensate the loss within a certain range by phase design (e.g., the $n = 1.5$ case in Fig. 2). Indeed, the phase can be retrieved by strictly deducing a proper source contribution to balance the propagation loss and thus achieve an exact intensity-preserved "lossless" SPP beam. According to earlier discussions, we introduce a source-to-beam density as $\rho \propto \frac{dx}{dz}$. Assuming an SPP with an attenuation length of l and a fixed intensity of the unit source, the beam intensity in the z axis contributed by a unit source can be expressed as

$$I_i \propto \exp\left(-\frac{r}{l}\right) = \exp\left(-\frac{x}{l\sin\theta}\right). \quad (3)$$

Thereafter, we can artificially tune the source-to-beam density to get a constant beam intensity as $I(z) = \rho I_i = c$. Then, we have the equation

$$\frac{dx}{dz}\exp\left(-\frac{x}{l\sin\theta}\right) = c. \quad (4)$$

Solving Eqs. (1), (2), and (4), we can obtain the phase distribution along the x axis for a loss compensated SPP beam. With the given $l = 15$ μm [7], a particular phase distribution is numerically retrieved to realize a straight lossless SPP beam as the calculation result shown in Fig. 5(a). Figure 5(c) depicts the retrieved phase distribution together with the previous $n = 1.5$ case for a comparison, which shows the lossless one has less curvature agreeing with less enhancement that is needed to balance the loss. Subsequently, we carried out the experiment by in-plane diffraction and successfully achieved this lossless beam as shown in Fig. 5(b), which almost reproduces the theoretical one. More clearly, Figs. 5(d) and 5(e) further depict the well achieved lossless profiles of the main lobe with a preserved intensity within a distance of $z < 35$ μm for both calculated and experimental results, respectively, which are in very good coincidence. Thus, an intensity-preserved and nearly nondiffracting SPP beam with strict design is well demonstrated.

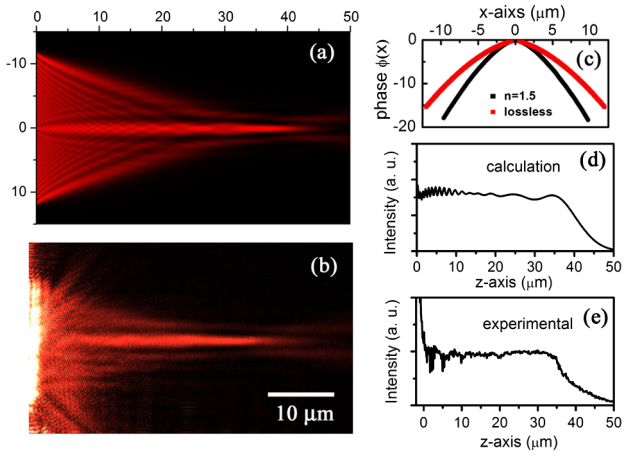

FIG. 5 (color online). Well achieved lossless SPP beams by (a) calculation and (b) experiment with a well designed phase distribution. (c) Retrieved phase distribution for the lossless beam compared with the previous $n = 1.5$ case. (d) Calculated and (e) experimental intensity profiles of the main lobes with respect to the beam of (a) and (b), respectively, revealing very good preserved intensity within a distance of ~ 35 μm.

It is reasonably believed that our design is capable of achieving almost any kind of intensity profile by introducing an arbitrary function of $F(z)$ as $I(z) = \rho I_u = cF(z)$ [e.g., an exponential increasing beam with $F(z) = \exp(\frac{z-z_0}{l'})$; see the Supplemental Material [24]], which would possibly imply particular applications (e.g., in optical trapping [25]). Notably, this designable scheme is valid not only for the lossy SPP but also for other beam systems as the item of $\exp(-r/l)$ in Eq. (3) is replaced by a more general function. In addition to these novelties, the achieved SPP beams retain other unique properties, e.g., the self-healing property, which was also experimentally observed (see the Supplemental Material [24]).

In summary, we have achieved a group of self-collimated SPP beams by symmetric phase modulation. A paradox between a nondiffracting versus linear focusing was proposed and insensitively studied. Utilizing an intuitive source-to-beam diagram, we successfully explained the nature of these beams. It is concluded that although some of these beams have a nondiffracting appearance, they are not the real ones except the particular case of $n = 1.0$. As a result of constructive diffractions, these SPP beams can be regarded as a kind of the focusing with respect to a line but not a point. This newly discovered source-to-beam relationship offers us a powerful and flexible method to design an intensity controllable beam, and an interesting lossless SPP beam is designed and realized as an example. Our study gives a unique insight into the collimated SPP beam formation and is expected to inspire more intriguing phenomena and potential applications in beam engineering and nanophotonic manipulations.

The authors would thank Q. J. Wang and X. N. Zhao for their help and support in the sample fabrications.

This work is supported by the State Key Program for Basic Research of China (Grants No. 2012CB921501, No. 2010CB630703, No. 2009CB930501, and No. 2011CBA00200), the National Natural Science Foundation of China (Grants No. 11174136, No. 10974090, No. 11021403, and No. 60990320), and PAPD of Jiangsu Higher Education Institutions.

*Corresponding author.
taoli@nju.edu.cn
http://dsl.nju.edu.cn/litao

[1] J. A. Schuller, E. S. Barnard, W. S. Cai, Y. C. Jun, J. S. White, and M. L. Brongersma, Nat. Mater. **9**, 193 (2010).
[2] G. A. Siviloglou, J. Broky, A. Dogariu, and D. N. Christodoulides, Phys. Rev. Lett. **99**, 213901 (2007).
[3] G. A. Siviloglou, J. Broky, A. Dogariu, and D. N. Christodoulides, Opt. Lett. **33**, 207 (2008).
[4] A. Salandrino and D. N. Christodoulides, Opt. Lett. **35**, 2082 (2010).
[5] P. Zhang, S. Wang, Y. M. Liu, X. B. Yin, C. G. Lu, Z. G. Chen, and X. Zhang, Opt. Lett. **36**, 3191 (2011).
[6] A. Minovich, A. Klein, N. Janunts, T. Pertsch, D. Neshev, and Y. Kivshar, Phys. Rev. Lett. **107**, 116802 (2011).
[7] L. Li, T. Li, S. Wang, C. Zhang, and S. Zhu, Phys. Rev. Lett. **107**, 126804 (2011).
[8] A. E. Klein, A. Minovich, M. Steinert, N. Janunts, A. Tünnermann, D. N. Neshev, Y. S. Kivshar, and T. Pertsch, Opt. Lett. **37**, 3402 (2012).
[9] E. Greenfield, M. Segev, W. Walasik, and O. Raz, Phys. Rev. Lett. **106**, 213902 (2011).
[10] L. Froehly, F. Courvoisier, A. Mathis, M. Jacquot, L. Furfaro, R. Giust, P. A. Lacourt, and J. M. Dudley, Opt. Express **19**, 16455 (2011).
[11] I. Kaminer, R. Bekenstein, J. Nemirovsky, and M. Segev, Phys. Rev. Lett. **108**, 163901 (2012).
[12] P. Zhang, Y. Hu, D. Cannan, A. Salandrino, T. Li, R. Morandotti, X. Zhang, and Z. Chen, Opt. Lett. **37**, 2820 (2012).
[13] P. Zhang, Y. Hu, T. Li, D. Cannan, X. Yin, R. Morandotti, Z. Chen, and X. Zhang, Phys. Rev. Lett. **109**, 193901 (2012).
[14] C. Zhao and J. S. Zhang, Opt. Lett. **34**, 2417 (2009).
[15] C. Zhao and J. S. Zhang, ACS Nano **4**, 6433 (2010).
[16] T. Tanemura, K. C. Balram, D. Ly-Gagnon, P. Wahl, J. S. White, M. L. Brongersma, and D. A. B. Miller, Nano Lett. **11**, 2693 (2011).
[17] L. Li, T. Li, S. M. Wang, S. N. Zhu, and X. Zhang, Nano Lett. **11**, 4357 (2011).
[18] J. Durnin, J. J. Micel, Jr., and J. H. Eberly, Phys. Rev. Lett. **58**, 1499 (1987).
[19] J. Lin, J. Dellinger, P. Genevet, B. Cluzel, F. de Fornel, and F. Capasso, Phys. Rev. Lett. **109**, 093904 (2012).
[20] M. V. Berry and N. L. Balazs, Am. J. Phys. **47**, 264 (1979).
[21] A. Drezet, A. Hohenau, D. Koller, A. Stepanov, H. Ditlbacher, B. Steinberger, F. R. Aussenegg, A. Leitner, and J. R. Krenn, Mater. Sci. Eng. B **149**, 220 (2008).
[22] A. Drezet, A. Hohenau, A. L. Stepanov, H. Ditlbacher, B. Steinberger, N. Galler, F. R. Aussenegg, A. Leitner, and J. R. Krenn, Appl. Phys. Lett. **89**, 091117 (2006).
[23] Y. Kaganovsky and E. Heyman, Opt. Express **18**, 8440 (2010).
[24] See Supplemental Material at http://link.aps.org/supplemental/10.1103/PhysRevLett.110.046807 for a diagram of the source-to-beam correspondence curves, a well-designed exponential increasing beam, and self-healing property.
[25] D. B. Ruffner and D. G. Grier, Phys. Rev. Lett. **109**, 163903 (2012).